AIMS Mathematics, 9(8): 23142–23157.
DOI: 10.3934/math.20241125
Received: 11 March 2024
Revised: 01 June 2024
Accepted: 05 June 2024
Published: 30 July 2024

http://www.aimspress.com/journal/Math

Research article

Biomedical importance of Casson nanofluid flow with silver and Fe_2O_3 nanoparticles delivered into a stenotic artery: Numerical study

Gunisetty Ramasekhar[1], Shaik Jakeer[2], Seethi Reddy Reddisekhar Reddy[3], Shalan Alkarni[4] and Nehad Ali Shah[5,*]

[1] Department of Mathematics, Rajeev Gandhi Memorial College of Engineering and Technology (Autonomous), Nandyal 518501, Andhra Pradesh, India
[2] School of Technology, The Apollo University, Chittoor, Andhra Pradesh 517127, India
[3] Department of Mathematics, Koneru Lakshmaiah Education Foundation, Bowrampet, Hyderabad, Telangana 500043, India
[4] Department of Mathematics, College of Sciences, King Saud University, P.O.Box 2455, Riyadh 11451, Saudi Arabia
[5] Department of Mechanical Engineering, Sejong University, Seoul 05006, South Korea

*** Correspondence:** Email: nehadali199@sejong.ac.kr.

Abstract: The blood flow over a stenotic artery is important investigation in mathematical fluid mechanics due to its significance in biomedical sciences. The present investigation aims to examine how nanoparticles affect circulation in a stenotic artery. We examine the significance of magnetized Casson nanofluid flow over a stenotic artery under consideration of the mathematical flow problem. By using the suitable self-similarity variables, the partial differential equation is transformed into ordinary differential equations. Then, the non-dimensional equations are solved using the MATLAB software in the Bvp5c scheme. By increasing the magnetic properties of the circulatory system's cells, which is a scheme that was previously utilized by raising the magnetic field parameter, there was a predictable decrease in the blood flow. Covering the stenosed artery with a greater amount of copper nanoparticles improves its heat transmission efficiency. The present technique may help distribute medications throughout the circulatory system.

Keywords: stenotic artery; Casson fluid; MHD; Bvp5c method; Fe_2O_3 and silver nanoparticles
Mathematics Subject Classification: 76A05, 76R05

Abbreviations: (x,r): Coordinates *(m)*; (u,v): Velocity components *(m/s)*; R: Radius of artery *(m)*; L_0: Length *(m)*; R_0: Width of unblocked region *(m)*; χ: Maximum height of stenosis; T,θ: Dimensional and dimensionless temperature (C^0); ϕ: Nanoparticles volume fraction; ψ: Stream function; η: Similarity index; γ: Curvature parameter; Pr: Prandtl number; τ_w: Wall shear stress; q_w: Heat flux; M: Magnetic field parameter; β: Casson fluid parameter

1. Introduction

Continuous investigation is being focused on nanofluids as a result of their remarkable thermal properties and the potential implications they may have in the field of medical research. Investigators have discovered that nanofluids contain the capacity to transmit heat more effectively than regular fluids, which highlights their ability to be used in place of traditional fluids. Several researchers have moved their attention to nanofluids due to their higher thermal efficiency. When compared to other fluids, nanoparticles are distinguished by their outstanding heat conductivity. This property makes them an important product across a wide variety of industries, including medicine, transport, gadgets, food choices, and nuclear power plants. Additionally, the incorporation of such nanoparticles, which vary in size between 1–100 nanometers, results in an increase in the conductive properties of the beginning fluids, which is in accordance with Choi (1995) [1]. The performance of nanoparticles in the field of biomedical science may be improved by enhancing their properties, which include dimensions, pharmacological content, and shape. The field of nanomedicine has seen tremendous advancements in the production of nanoparticles for many applications, with certain nanoparticles showing great potential in the management and surveillance of diseases. Researchers are always looking for new ways to use the properties of iron oxide for diagnostics and medications, which has led to its continuous use in medicine. A comprehensive investigation into the security, physiological reliability, and long-term impacts of these nanoparticles is required prior to when they are utilized for medical devices. It is of the utmost importance to underline this fact. Fe_2O_3 and Fe_3O_4 particles are magnetic resonance imaging (MRI) contrast mediums. The magnetic characteristics of Fe_2O_3 and Fe_3O_4 particles improve contrast in MRI pictures, which, in turn, enables an improved view of anomalies within organs and cells. When it comes to the administration of medications, Fe_2O_3 and Fe_3O_4 nanoparticles have the potential to serve as transporters. There is the potential to attach medicinal substances to the outside of iron oxide particles via the procedure of the functionalization processes. To facilitate the administration of drugs in a targeted manner, the nanoparticles may be directed to specific targets using magnetic fields from the outside [2–5].

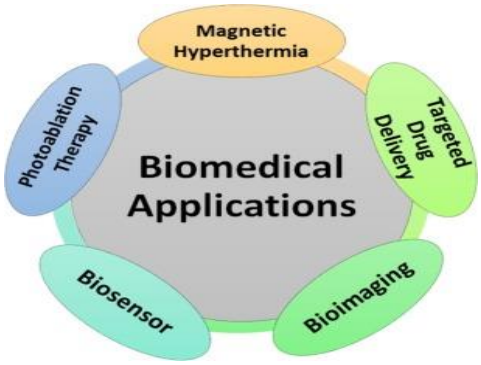

Figure 1. Diagram demonstrating nanoparticle biomedical uses.

To deliver chemotherapeutic medications into tumor locations without causing damage to adjacent living cells targeted drug administration is an essential component in the field of bioscience. Currently, the principal source of magnetic substances that have been employed for the delivery of chemotherapeutic medicines to particular regions are nanoparticles comprised of ferrous oxide. For the objective of achieving this goal, several chemicals have been used. The utilization of tiny particles in a magnetic thermal treatment is an important application in the field of biology. In the process of hyperthermia, which is also known as magnetic treatment, tumors are heated to temperatures above 42 degrees Celsius to eradicate cancerous tumor cells. One advantage of this method over chemotherapy treatments is that it focuses on the tumor without harming the adjacent healthy tissue, which is presented in Figure 1.

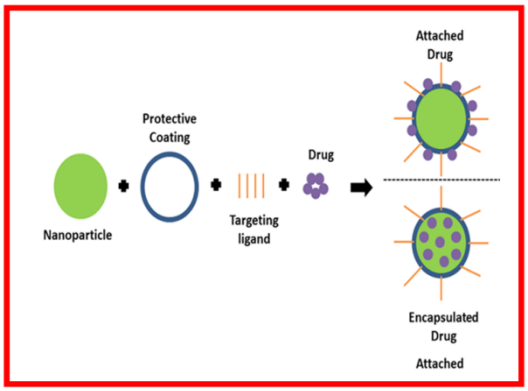

Figure 2. Diagram demonstrating nanoparticle focused drug delivary.

When radiation is administered, anticancer drugs are transported to tumors via the bloodstream. Both an inadequate specificity and hazardous effects, which have the potential to cause damage to normal cells and tissues, are examples of adverse responses that might occur while using this medicine. Therefore, the use of individualized medicine distribution as an alternative to radiation has been investigated. In order to maximize the delivery of medicines to the tumor site while limiting any adverse effects, focused drug administration has been used. Focused drug administration involves the exact placement of the medicine using magnets. Magnets may be coated with valuable metals or polymer substances to enable either a combination or the absorption of drugs, as demonstrated in

Figure 2 [6–9].

Arterial stenosis is a disorder that is rather common across the human circulation vascular circuit and is associated with a number of other conditions. Additionally, there is a significant prevalence of blocks or narrowing of the blood vessels. A disturbance takes place in the usual path of circulation through the vessel as a consequence of the constriction that takes place. Nanotechnology is a field of science that spans a vast variety of different concepts and issues. Drug delivery systems tailored to the treatment of pharmaceuticals have been the mainstay of the latest developments in nanotechnologies. These systems are artificially nanometer-sized. Each of the various kinds of service delivered drug delivery methods, including nano-emulsions and microscopic particles, exhibit a wide range of favorable qualities [10]. They provide a variety of advantages to the person who uses them. In addition, they have a number of issues that are problematic. Therefore, every mechanism has been developed as a solution for the deficiencies of the framework that came before it [11–14].

1.1. Inspiration

Heart disorders are an important contributor to fatalities and medical conditions that occur in a large number of individuals worldwide. Medical professionals and members of the scientific community are having trouble understanding out how to address these health issues. Atherosclerosis, which is the accumulation of cholesterol in the artery walls, is a prevalent cardiovascular condition that may lead to stenosis, which is the shrinking of the arterial walls and a reduction in the movement of blood. This research work attempts to investigate how many factors influence how a particular substance moves through a tiny region of the human body known as an artery. This study accounts for the circulation of blood, the biological reactions that take place throughout it, and the rate at which the blood flows.

1.2. Novelty

This study shows a unique feature of blood circulation as it investigates how biological reactions and circulation rates affect the suggested blood movement within arteries. This is an innovative approach to improve blood circulation in narrowed arterial walls, which could improve the passage of blood across narrowed or obstructed arteries. Furthermore, the main purpose of this study is to evaluate the significance of iron oxide and silver nanoparticles that are inserted into the bloodstream via arteries that have been stenosed. In this section, we explore the impacts of several factors, such as the magnetohydrodynamic (MHD) flow and Casson fluids. By considering the features of heat transmission that the bio-nanofluid possesses we can establish a more thorough understanding of the intricate fluid dynamics that occur in stenosed artery vessels.

2. Mathematical formulation of the problem

1) In the current problem, we considered that blood acts under an incompressible steady fluid flow through an arterial stenosis of length $L_0/2$.

2) The coordinate system is selected in such a way that the blood flow along the $x-axis$ and the $r-axis$ are taken perpendicular to the blood flow.
3) Figure 3 shows a schematic figure of the governing model, which takes these parameters into consideration.

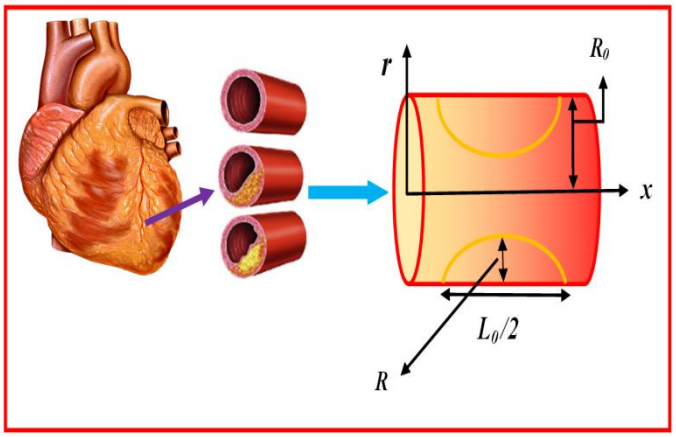

Figure 3. The artery's physical structure.

4) The blood flow through an artery with a stenosis of a cosine shape constriction has a width of $2R_0$ for the unobstructed region, where $R(x)$ is radius of the artery and χ is the maximum height of stenosis.
5) The profile for the stenosed region is as follows:

$$\frac{R(x)}{R_0}=\begin{cases}1-\dfrac{\chi}{2}\left(1+\mathrm{Cos}\left(\dfrac{4\pi x}{L_0}\right)\right), & -\dfrac{L_0}{4}<x<\dfrac{L_0}{4}=R_0\\ 1 & ,otherwise\end{cases} \tag{1}$$

6) It is possible to formulate the stable boundary layer equations that regulate the temperature transfer and flow for non-Newtonian nanofluids as follows [15–17]:

$$\frac{\partial(ru)}{\partial x}+\frac{\partial(rv)}{\partial r}=0, \tag{2}$$

$$u\left(\frac{\partial}{\partial x}+v\frac{\partial}{\partial r}\right)u=\frac{\mu_{nf}}{\rho_{nf}}\left(1+\frac{1}{\beta}\right)\frac{\partial}{r\partial r}\left(r\frac{\partial u}{\partial r}\right)-\frac{\sigma_{nf}B^2}{\rho_{nf}}u, \tag{3}$$

$$\left(u\frac{\partial}{\partial x}+v\frac{\partial}{\partial r}\right)T=\frac{k_{nf}}{\left(\rho C_p\right)_{nf}}\frac{\partial}{r\partial r}\left(r\frac{\partial T}{\partial r}\right). \tag{4}$$

The suitable boundary conditions that correspond with the fluid flow regime are considered as follows [16,17]:

$$\left.\begin{array}{ll} u = u_0, v = 0 \text{ and } T = T_w & at \;\; r = R(x), \\ u \to 0, \text{and } T \to T_\infty & as \; r \to \infty. \end{array}\right\} \tag{5}$$

The mathematical models for the thermophysical properties of the nanofluid are as follows:

$$Y_1 = \frac{\mu_{nf}}{\mu_f}, Y_2 = \frac{\rho_{nf}}{\rho_f}, Y_3 = \frac{\sigma_{nf}}{\sigma_f}, Y_4 = \frac{(\rho c_p)_{nf}}{(\rho c_p)_f}, Y_5 = \frac{k_{nf}}{k_f} \tag{6}$$

The continuity Eq (1) can be satisfied by introducing the stream function ψ for u and v such that

$$u = \frac{1}{r}\frac{\partial \psi}{\partial r}, v = -\frac{1}{r}\frac{\partial \psi}{\partial x} \tag{7}$$

Then, Eqs (3) and (4) are converted as follows:

$$\frac{1}{r}\frac{\partial \psi}{\partial r}\frac{\partial}{\partial x}\left(\frac{1}{r}\frac{\partial \psi}{\partial r}\right) - \frac{1}{r}\frac{\partial \psi}{\partial x}\frac{\partial}{\partial r}\left(\frac{1}{r}\frac{\partial \psi}{\partial x}\right) = \frac{\mu_{nf}}{\rho_{nf}}\left(1 + \frac{1}{\beta}\right)\frac{\partial}{r\partial r}\left(\frac{\partial^2 \psi}{\partial r^2} - \frac{1}{r}\frac{\partial \psi}{\partial r}\right) - \frac{\sigma_{nf} B^2}{\rho_{nf}}\frac{1}{r}\frac{\partial \psi}{\partial r}, \tag{8}$$

$$\left(\frac{1}{r}\frac{\partial \psi}{\partial r}\right)\frac{\partial T}{\partial x} - \left(\frac{1}{r}\frac{\partial \psi}{\partial x}\right)\frac{\partial T}{\partial r} = \frac{k_{nf}}{\left(\rho C_p\right)_{nf}}\frac{\partial}{r\partial r}\left(r\frac{\partial T}{\partial r}\right). \tag{9}$$

The suitable self-similarity transformations are as follows:

$$\left.\begin{array}{l} u = \dfrac{u_0 x}{L_0} f'(\eta), \\ v = -\dfrac{R}{r}\sqrt{\dfrac{u_0 \upsilon_f}{L_0}} f(\eta), \qquad \eta = \dfrac{r^2 - R^2}{2R}\sqrt{\dfrac{u_0}{\upsilon_f L_0}}. \\ \theta(\eta) = \dfrac{T - T_\infty}{T_w - T_\infty} \end{array}\right\} \tag{10}$$

After applying the self-similarity variables, Eqs (8) and (9) take the following form:
The non-dimensional form of Eq (1) is as follows:

$$\begin{array}{l} f = 1 - \dfrac{\varepsilon}{2}\left(1 + \text{Cos}\left(4\pi x\right)\right), \quad -\dfrac{1}{4} < x < \dfrac{1}{4} \\ = 1 \end{array} ,$$

where $f = \dfrac{R(x)}{R_0}$ *and* $\varepsilon = \dfrac{\chi}{R_0}$ are the dimensionless measures of stenosis in the reference artery.

$$\frac{1}{Y_1 Y_2}\left[\left(1 + 2\gamma\eta\right)\left(1 + \frac{1}{\beta}\right)f''' + 2\gamma f''\right] + ff'' - f'^2 - \frac{Y_3}{Y_2}Mf' = 0, \tag{11}$$

$$\frac{Y_5}{Y_4}\frac{1}{Pr}\left[\left(1+2\gamma\eta\right)\theta''+2\gamma\theta'\right]+f\theta'-f'\theta=0. \tag{12}$$

The non-dimensional boundary conditions are as follows:

$$\left.\begin{aligned}\eta=0 &: f\left(\eta\right)=0,\ f'\left(\eta\right)=1,\theta\left(\eta\right)=1,\\ \eta\to\infty &: f'\left(\eta\right)\to 0,\theta\left(\eta\right)\to 0.\end{aligned}\right\} \tag{13}$$

Where $Pr=\dfrac{k_f}{\left(\mu C_p\right)_f}$ is the Prandtl number, $\gamma=\sqrt{\dfrac{\upsilon_f L_0}{u_0 R^2}}$ is Curvature parameter, and $M=\dfrac{\sigma_f B^2 L_0}{u_0\rho_f}$ is the Magnetic parameter.

The dimensional form of the skin-friction coefficient and the Nusselt numbers are defined as follows:

$$C_f=\left(1+\frac{1}{\beta}\right)\frac{2\tau_w}{\rho_f U_w^2}, \tag{14}$$

where the shear stress τ_w is

$$\tau_w=\mu_{nf}\left.\frac{\partial u}{\partial r}\right|_{r=R}.$$

$$Nu=\frac{xq_w}{k_f\left(T_w-T_\infty\right)}, \tag{15}$$

where the heat flux q_w is

$$q_w=-k_{nf}\left.\frac{\partial T}{\partial r}\right|_{r=R}.$$

The non-dimensional form of Eqs (14) and (15) converts to the following:

$$Re_r^{1/2}C_f=Y_1\left(1+\frac{1}{\beta}\right)f''\left(0\right), \tag{16}$$

$$Re_r^{-1/2}Nu_r=-\frac{k_{nf}}{k_f}\theta'\left(0\right). \tag{17}$$

Where Re_r is the local Reynolds number.

Table 1. The thermophysical characteristic of blood and nanoparticles [18,19].

Property	**Blood**	**Fe_2O_3**	**Silver**
Density $\rho\ (kgm^{-3})$	1050	5180	10,500
Specific heat $C_p\ (Jkg^{-1}K^{-1})$	3617	670	235
Heat conductivity $k_f\ (Wm^{-1}K^{-1})$	0.52	9.7	429
Electrical conductivity $\sigma\ (\Omega m)^{-1}$	0.8	25000	63×10^{-6}
Prandtl number	21		

3. Solution methodology

The nature of the ordinary differential equation (ODE) system (11–12) with boundary conditions (BCs) (13) is extremely nonlinear in its characteristics. For the purpose of dealing with these equations, we adopt a computational approach known as the Bvp5c method. Using the MATLAB software, we are able to solve the control problem. The midway method's standard operating procedure is laid out in detail in Figure 4.

$$f''' = \frac{1}{(1+2\gamma\eta)\left(1+\frac{1}{\beta}\right)\frac{1}{Y_1Y_2}}\left[\frac{1}{Y_1Y_2}2\gamma f'' + ff'' - f'^2 - \frac{Y_3}{Y_2}Mf'\right], \tag{18}$$

$$\theta'' = \frac{1}{(1+2\gamma\eta)\frac{Y_5}{Y_4}\frac{1}{Pr}}\left[\frac{Y_5}{Y_4}\frac{1}{Pr}2\gamma\theta' + f\theta' - f'\theta\right]. \tag{19}$$

The non-dimensional boundary conditions are as follows:

$$\left.\begin{aligned} &\eta = 0 : f(\eta) = 0,\ f'(\eta) = 1, \theta(\eta) = 1, \\ &\eta \to \infty : f'(\eta) \to 0, \theta(\eta) \to 0. \end{aligned}\right\} \tag{20}$$

The following steps of the shooting scheme are provided as follows:

$$f = R_1,\ f' = R_2,\ f'' = R_3,\ f''' = R_3',\ \theta = R_4, \theta' = R_5, \theta'' = R_5',$$

$$R_1' = R_2$$
$$R_2' = R_3$$
$$R_3' = -\left[\frac{1}{(1+2\gamma\eta)\left(1+\frac{1}{\beta}\right)\frac{1}{X_1X_2}}\left[\frac{1}{X_1X_2}2\gamma R_3 + RR_3 - (R_2)^2 - \frac{X_3}{X_2}MR_2\right]\right]$$
$$R_4' = R_5$$
$$R_5' = -\left[\frac{1}{(1+2\gamma\eta)\frac{X_5}{X_4}\frac{1}{Pr}}\left[\frac{X_5}{X_4}\frac{1}{Pr}2\gamma R_5 + RR_5 - R_2R_4\right]\right].$$

Moreover, the boundary conditions are as follows:

$$\left.\begin{aligned} R_1(\eta) = 0,\ R_2(\eta) = 1,\ R_4(\eta) = 1,\ at\ \eta = 0 \\ R_2(\eta) \to 0,\ R_4(\eta) \to 0\ \ as\ \eta \to \infty. \end{aligned}\right\}$$

When performing the inner iteration, the criteria for convergence are consistently employed. For the present investigation, a relative tolerance of error 10^{-8} is taken into account.

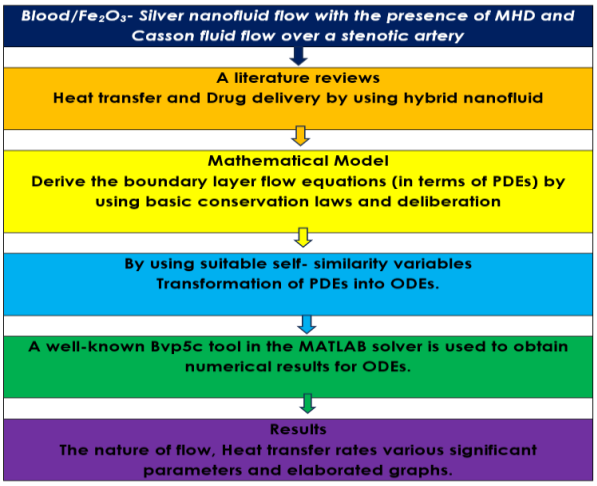

Figure 4. Flow chart of the present investigation problem.

4. Results and discussion

In order to describe the performance of the Casson nanofluid flow over a stenotic artery the numerical technique was utilized to obtain the necessary solution to the modified, highly non-linear coupled equations. The present examination followed by various important active parameters, along with the BVP5c process in MATLAB solver, was used in this investigation phase. The Figures demonstrate the influence of numerous important factors within these ranges: $0.1 < M < 0.5,\ 0.2 < \gamma < 0.6,\ 0.3 < \beta < 0.9, 2.0 < Pr < 4.0$. We evaluated the parameter values and

considered 21 as the Prandtl number for Blood for the two different cases of nanofluids considered. A velocity and temperature profile shows several important parameters. Figure 5 (a) displays the effect of magnetic field parameter on the velocity profile where there is a decreasing nature on the velocity profile for the greater values of *M*. Physically, when *M* increases, it generates a Lorentz force, which slows the fluid flow. Because the Lorentz force opposes the fluid movement, the velocity flow diminutions as a result of the additional resistance, resulting in a reduction in the velocity field. A representation of the influence of the curvature parameter γ on velocity outline is shown in Figure 5 (b). The velocity outline is increased as the values of γ increase. Physically, when the arterial walls decrease due to the stenosis, the blood vessel's curvature changes. This occurrence comes the possibility of changes to the blood circulation and related trends, which might have an important physiological significance. Additionally, a similar trend is seen for the energy profile, which is presented in Figure 6 (a). It is important to remember how the non-Newtonian nature of the Casson fluid, which is also called a viscoelastic liquid, depends on the amount of the Casson fluid parameter. The fluid behaves like a fluid that obeys Newton's laws, and its movement rate rises as the Casson fluid parameter grows because the shear stress is greater than the yield stress. The figure shows that when the Casson fluid parameter values increase, the velocity profile decreases. Primarily, this is accomplished because the fluid behaves like a Newtonian flow as the Casson factor becomes substantial. A higher Casson parameter reduces the stress induced by the yield, thus restricting the fluid's movement, which is shown in Figure 5 (c). Figure 6 (b) depicts the influence of the *Pr* number where an increase in the *Pr* number values is linked to a decrease in the energy profile. The value of the *Pr* number has an opposite relationship to the temperature diffusivity. When the Prandtl value is over estimated, the heat diffusion decreases, which makes the heat dispersion worse. If the Prandtl number increases, the heat dispersion will typically decrease. The inner layers of the arteries are very constricted, which makes it difficult for blood to flow across the arteries. One possible inference is the fact that heat diffusion is less than the velocity dispersion, which considers a larger value of the Prandtl number. The illustration clearly demonstrates that the thermal boundary barrier thins out as the particle concentration increases from 2.0 to 4.0.

4.1. Contour profiles for Skin friction and Nusselt number

The effect of a Casson fluid and the magnetic field parameters on skin friction outline is demonstrated in Figure 7 (a). For higher values of the Casson fluid parameter, the skin friction profile decreases due to the physical phenomenon; consequently, the heat diffusion decreases, which makes the heat dispersion worse. This leads to a greater amount of power through movement. We noticed an opposing trend on Nusselt number outline, which is presented in Figure 7 (b).

4.2. Streamlines and velocity contour profiles

Streamlines, which are the exploration of fluid action and the representation of flow, provide a variety of properties that, whenever combined, make them great instruments to perform research and analyses on the motions of fluids. The streamlines are particularly useful for this purpose. This is particularly true when used to investigate fluid movements. Figures 8 (a) and (b) are streamlines plots that exhibit the magnetic parameters for various values. The magnetic parameter strength draws electrical conductivity molecules increasingly towards to the main stream; moreover, the velocity

contour is presented in Figure 8 (c).

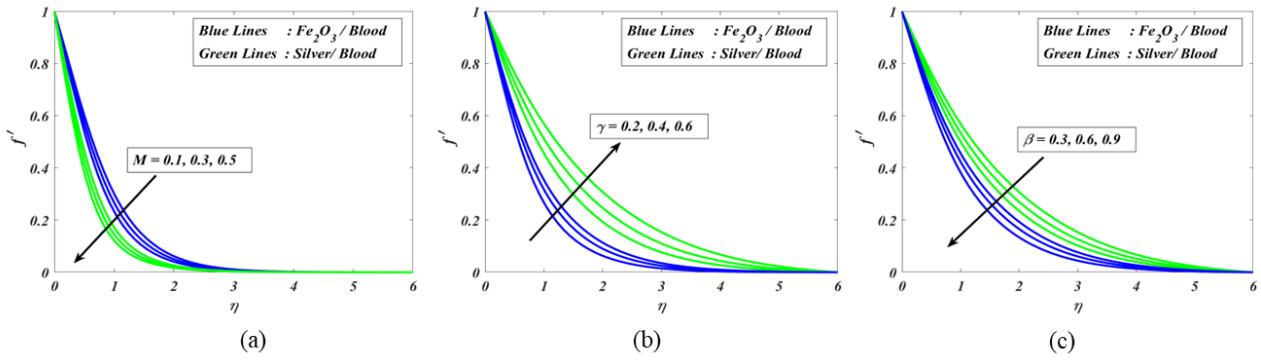

Figure 5. (a) Variation due to M on $f'(\eta)$, (b) Variation due to γ on $f'(\eta)$, (c) Variation due to β on $f'(\eta)$.

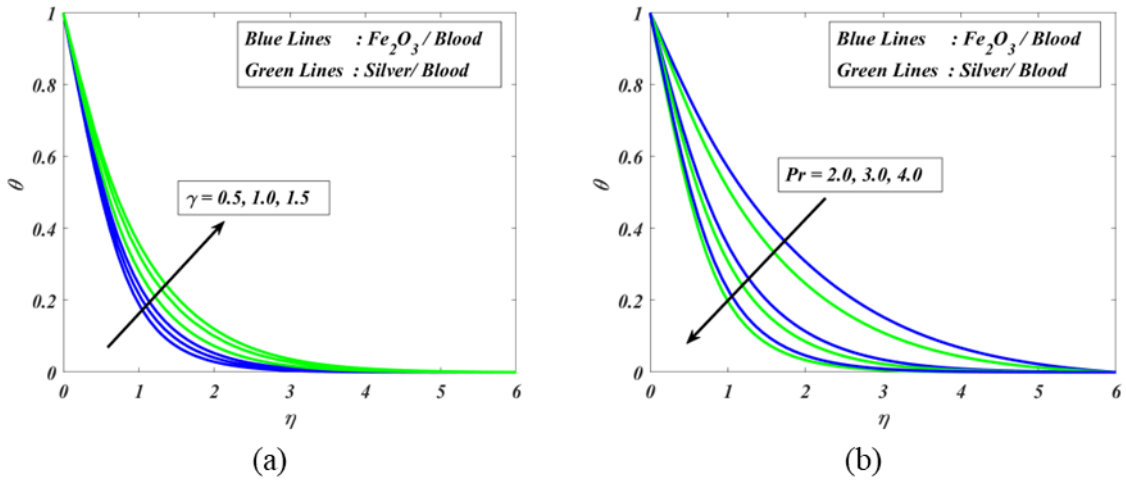

Figure 6. (a) Variation due to γ on $\theta(\eta)$, (b) Variation due to Pr on $\theta(\eta)$.

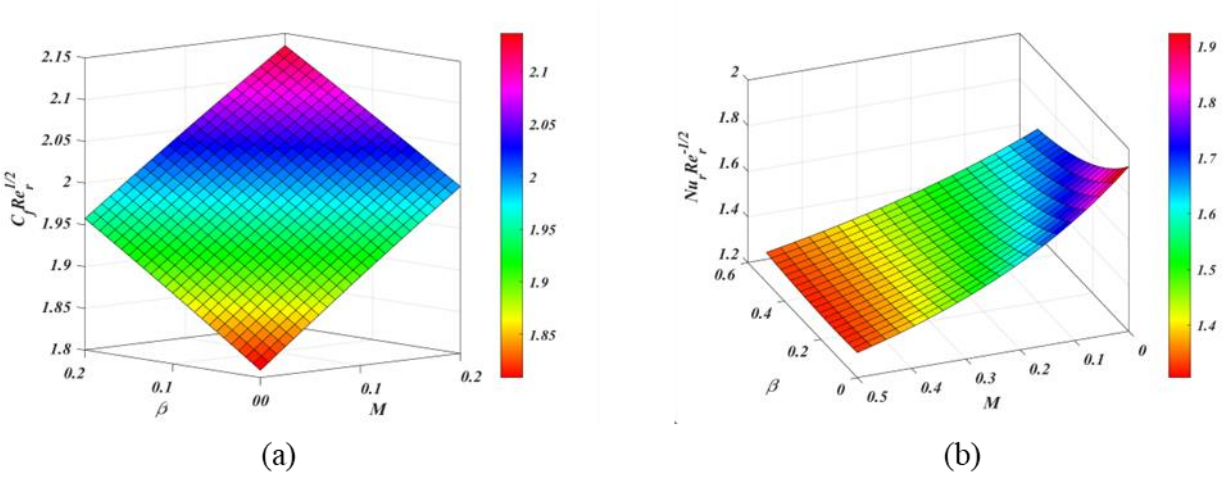

Figure 7. (a) Impact of β and M for $C_f Re_r^{0.5}$, (b) Impact of β and M for $Nu_r Re_r^{-0.5}$.

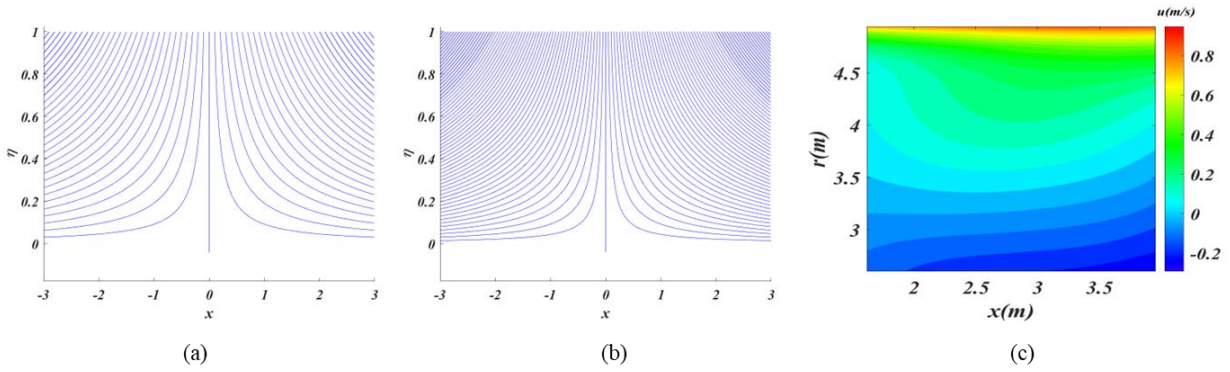

Figure 8. (a) Streamline effects for $M = 0.5$, (b) $M = 1.0$, (c) Velocity contours for the velocity along *x*-direction.

Table 2. Comparision results for $C_f Re_r^{1/2}$ for various values of γ *and* ϕ_1 [15].

Waqas et al.		Present outcomes (bvp5c)
γ, ϕ_1	$C_f Re_r^{1/2}$	$C_f Re_r^{1/2}$
0.1, 0.01	0.939968	0.939915
0.12, 0.01	0.924794	0.924746
0.14, 0.01	0.911311	0.911300
0.1, 0.05	1.329552	1.329536
0.1, 0.1	1.175985	1.175992

5. Conclusions

This study presented an investigation of the movement of a magnetized Casson nanofluid across a stenotic artery. The partial differential equations (PDEs) of the mathematical system were

transformed into the corresponding ODEs that illustrated the flow of the problem. The resulting equations were graphically drawn by employing the Bvp5c approach in MATLAB software.

The point wise conclusions are as follows:

1) This research advances our knowledge of heat transfers in challenging fluids, which paves the way for future studies of bio-nanofluid behavior.
2) Enhancing the magnetic field inputs resulted in a decreased behavior of the velocity profile.
3) The profile of the nanofluid velocity was improved for when the curvature parameter values increased.
4) Additional properties of the curvature parameter inputs resulted in an improved temperature profile.
5) A decrease in fluid temperature profile was caused by an increase in the *Pr* number values.
6) In this model, the skin friction and Nusselt number profiles were increased at higher values of the magnetic field parameter.

5.1. Limitations of the present study

There are several possible limitations that may were encountered in this research, which could have an impact on the depth, accuracy, and predictability of the results. Examples of such limitations involve the following:

1) The computational methods used to calculate the governing equations had constraints, including convergence difficulties, which affected the modeling reliability and precision.
2) Assumptions concerning the thermophysical characteristics of bio-nanofluids did not fully reflect real-world circumstances, since they changed with concentration and temperature.
3) The absence of experimental data for testing made it more difficult to validate the reliability of the framework and to determine whether or not it is applicable to circumstances that occur in real life.
4) Considering that the research included assumptions about particular boundary conditions that could not be totally practical for some settings, there was a possibility that the mathematical framework and the real experimental initiates differed from one another.

5.2. Feature work

Within the scope of the ongoing investigation, the following are some possible proposals for further studies:

1) The effect of magnetic fields can be evaluated with different non-Newtonian fluids such as Carreau fluids, Casson fluids, Williamson fluids, and Sisko fluids.
2) In further studies, it is possible that the theoretical conclusions will be validated through the use of experimental investigations.
3) There is a possibility of conducting research to discover the computational solution of a multi-phase problem.
4) The theoretical framework might be solved through the use of an artificial neural network (ANN).
5) There is a possibility to determine the parameters that are most effective in boosting the heat transport and chemical interactions.

6) The focus of future applications will focus on individualized therapies that consider the unique characteristics of each patient.

Author contributions

Gunisetty Ramasekhar: Conceptualization; Data curation; Writing–original draft; Shaik Jakeer: Conceptualization; Writing–review & editing; Seethi Reddy Reddisekhar Reddy: Methodology; Shalan Alkarni: Data curation; Formal Analysis; Methodology; Software; Writing–review & editing; Nehad Ali Shah: Conceptualization; Investigation; Methodology; Validation; Writing–review & editing. All authors have read and agreed to the published version of the manuscript.

Use of AI tools declaration

The authors declare they have not used Artificial Intelligence (AI) tools in the creation of this article.

Acknowledgments

This project was supported by Researchers Supporting Project number (RSPD2024R909), King Saud University, Riyadh, Saudi Arabia.

Conflict of interest

All authors declare no conflicts of interest in this paper.

References

1. S. U. S. Choi, Enhancing Thermal Conductivity of Fluid with Nanoparticles, 1995. Available from: https://www.osti.gov/biblio/196525.
2. K. McNamara, S. A. M. Tofail, Nanoparticles in biomedical applications, *Adv. Phys. X*, **2** (2017), 54–88. https://doi.org/10.1080/23746149.2016.1254570
3. L. Sarwar, A. Hussain, Flow characteristics of Au-blood nanofluid in stenotic artery, *Int. Commun. Heat Mass Transfer*, **127** (2021), 105486. https://doi.org/10.1016/j.icheatmasstransfer.2021.105486
4. M. Yaseen, S. K. Rawat, N. A. Shah, M. Kumar, S. M. Eldin, Ternary Hybrid Nanofluid Flow Containing Gyrotactic Microorganisms over Three Different Geometries with Cattaneo–Christov Model, *Mathematics*, **11** (2023), 1237. https://doi.org/10.3390/math11051237
5. R. S. Varun Kumar, P. Gunderi Dhananjaya, R. Naveen Kumar, R. J. Punith Gowda, B. C. Prasannakumara, Modeling and theoretical investigation on Casson nanofluid flow over a curved stretching surface with the influence of magnetic field and chemical reaction, *Int. J. Comput. Methods Eng. Sci. Mech.*, **23** (2022), 12–19. https://doi.org/10.1080/15502287.2021.1900451

6. N. A. Shah, A. Wakif, R. Shah, S. Yook, B. Salah, Y. Mahsud, et al., Effects of fractional derivative and heat source/sink on MHD free convection flow of nanofluids in a vertical cylinder: A generalized Fourier's law model, *Case Stud. Therm. Eng.*, **28** (2021), 101518. https://doi.org/10.1016/j.csite.2021.101518
7. R. Gunisetty, P. B. A. Reddy, A. Divya, Entropy generation analysis on EMHD non-Newtonian hybrid nanofluid flow over a permeable rotating disk through semi analytical and numerical approaches, *Proc. Inst. Mech. Eng. Part E J. Process Mech. Eng.*, 2023. https://doi.org/10.1177/09544089231199640
8. H. T. Basha, R. Sivaraj, Entropy generation of peristaltic Eyring–Powell nanofluid flow in a vertical divergent channel for biomedical applications, *Proc. Inst. Mech. Eng. Part E J. Process Mech. Eng.*, **235** (2021), 1575–1586. https://doi.org/10.1177/09544089211013926
9. S. R. Reddisekhar Reddy, S. Jakeer, V. E. Sathishkumar, H. T. Basha, J. Cho, Numerical study of TC4-NiCr/EG+Water hybrid nanofluid over a porous cylinder with Thompson and Troian slip boundary condition: Artificial neural network model, *Case Stud. Therm. Eng.*, **53** (2023), 103794. https://doi.org/10.1016/j.csite.2023.103794
10. K. Ur Rehman, N. Ul Saba, M. Y. Malik, I. Zehra, Nanoparticles individualities in both Newtonian and Casson fluid models by way of stratified media: A numerical analysis, *Eur. Phys. J. E*, **41** (2018), 37. https://doi.org/10.1140/EPJE/I2018-11641-8
11. M. Al Nuwairan and B. Souayeh, Simulation of Gold Nanoparticle Transport during MHD Electroosmotic Flow in a Peristaltic Micro-Channel for Biomedical Treatment, *Micromachines*, **13** (2022), 374. https://doi.org/10.3390/mi13030374
12. S. Jakeer, N. Shanmugapriyan, S. R. Reddisekhar Reddy, Numerical simulation of bio-magnetic nanofluid flow in the human circulatory system, *Numer. Heat Transfer Part A: Appl.*, 2024, 1–29. https://doi.org/10.1080/10407782.2024.2304046
13. M. M. Bhatti, O. A. Bég, M. M. Bhatti, O. A. Bég, S. I. Abdelsalam, Computational framework of magnetized MgO–Ni/water-based stagnation nanoflow past an elastic stretching surface: Application in solar energy coatings, *Nanomaterials*, **12** (2022), 1049. https://doi.org/10.3390/nano12071049
14. G. Ramasekhar, Scrutinization of BVP Midrich Method for Heat Transfer Analysis on Various Geometries in the Presence of Porous Medium and Thermal Radiation, **13** (2024), 100–107. https://doi.org/10.1166/jon.2024.2130
15. H. Waqas, U. Farooq, D. Liu, M. Alghamdi, S. Noreen, T. Muhammad, Numerical investigation of nanofluid flow with gold and silver nanoparticles injected inside a stenotic artery, *Mater. Des.*, **223** (2022), 111130. https://doi.org/10.1016/j.matdes.2022.111130
16. T. Sajid, W. Jamshed, M. R. Eid, G. C. Altamirano, F. Aslam, A. M. Alanzi, et al., Magnetized Cross tetra hybrid nanofluid passed a stenosed artery with nonuniform heat source (sink) and thermal radiation: Novel tetra hybrid Tiwari and Das nanofluid model, *J. Magn. Magn. Mater.*, **569** (2023), 170443 .https://doi.org/10.1016/j.jmmm.2023.170443
17. S. Z. Hussain Shah, A. Ayub, U. Khan, A. Darvesh, E.-S. M. Sherif, I. Pop, Thermal transport exploration of ternary hybrid nanofluid flow in a non-Newtonian model with homogeneous-heterogeneous chemical reactions induced by vertical cylinder, *Adv. Mech. Eng.*, **16** (2024), 16878132241252229. https://doi.org/10.1177/16878132241252229

18. C. G. Njingang Ketchate, P. Tiam Kapen, D. Fokwa, G. Tchuen, Stability analysis of non-Newtonian blood flow conveying hybrid magnetic nanoparticles as target drug delivery in presence of inclined magnetic field and thermal radiation: Application to therapy of cancer, *Inf. Med. Unlocked*, **27** (2021), 100800. https://doi.org/10.1016/j.imu.2021.100800
19. G. Ramasekhar, P. B. A. Reddy, Entropy generation on EMHD Darcy-Forchheimer flow of Carreau hybrid nano fluid over a permeable rotating disk with radiation and heat generation : Homotopy perturbation solution, *Proc. Inst. Mech. Eng. Part E J. Process Mech. Eng*, **237** (2023), 1179–1191. https://doi.org/10.1177/09544089221116575